Fermi National Accelerator Laboratory

A Limit on $\nu_\mu(\bar{\nu}_\mu) \to \nu_\tau(\bar{\nu}_\tau)$ Oscillations from a Precision Measurement of Neutrino-Nucleon Neutral Current Interactions

K.S. McFarland et al.

Fermi National Accelerator Laboratory
P.O. Box 500, Batavia, Illinois 60510

June 1995

Disclaimer

A Limit on $\nu_\mu(\overline{\nu}_\mu) \to \nu_\tau(\overline{\nu}_\tau)$ Oscillations from a Precision Measurement of Neutrino-Nucleon Neutral Current Interactions

K. S. McFarland[5], D. Naples[5], C. G. Arroyo[4], P. Auchincloss[8], P. de Barbaro[8]

A. O. Bazarko[4], R. H. Bernstein[5], A. Bodek[8], T. Bolton[6], H. Budd[8], J. Conrad[4],

R. B. Drucker[7], D. A. Harris[8], R. A. Johnson[3], J. H. Kim[4], B. J. King[4], T. Kinnel[9],

G. Koizumi[5], S. Koutsoliotas[4], M. J. Lamm[5],W. C. Lefmann[1], W. Marsh[5],C. McNulty[4],

S. R. Mishra[4], P. Nienaber[10], M. Nussbaum[3], M. J. Oreglia[2], L. Perera[3], P. Z. Quintas[4],

A. Romosan[4], W. K. Sakumoto[8], B. A. Schumm[2], F. J. Sciulli[4], W. G. Seligman[4],

M. H. Shaevitz[4], W. H. Smith[9], P. Spentzouris[4], R. Steiner[1], E. G. Stern[4],

M. Vakili[3],U. K. Yang[8],

[1] *Adelphi University, Garden City, NY 11530*

[2] *University of Chicago, Chicago, IL 60637*

[3] *University of Cincinnati, Cincinnati, OH 45221*

[4] *Columbia University, New York, NY 10027*

[5] *Fermi National Accelerator Laboratory, Batavia, IL 60510*

[6] *Kansas State University, Manhattan, KS 66506*

[7] *University of Oregon, Eugene, OR 97403*

[8] *University of Rochester, Rochester, NY 14627*

[9] *University of Wisconsin, Madison, WI 53706*

[10] *Xavier University, Cincinnati, OH 45207*

(June 16, 1995)

Abstract

We present a limit on $\nu_\mu(\overline{\nu}_\mu) \to \nu_\tau(\overline{\nu}_\tau)$ oscillations based on a study of inclusive νN interactions performed using the CCFR massive coarse grained detector in the FNAL Tevatron Quadrupole Triplet neutrino beam. The sensitivity to oscillations is from the difference in the longitudinal energy deposition pattern of $\nu_\mu N$ versus $\nu_\tau N$ charged current interactions. The ν_μ energies ranged from 30 to 500 GeV with a mean of 140 GeV. The minimum and maximum ν_μ flight lengths are 0.9 km and 1.4 km respectively. The lowest 90% confidence upper limit in $\sin^2 2\alpha$ of 2.7×10^{-3} is obtained at $\Delta m^2 \sim 50$ eV^2. This result is the most stringent limit to date for $25 < \Delta m^2 < 90$ eV^2.
14.60.Pq, 13.15.+g, 12.15.Mm

Typeset using REVTEX

The mixing of non-degenerate neutrino mass eigenstates would lead to oscillations of one neutrino type into another. For mixing between two generations, the oscillation probability is

$$P(\nu_1 \rightarrow \nu_2) = \sin^2 2\alpha \sin^2 \left(\frac{\Delta m^2 L}{E_\nu} \times 1.27 \frac{\text{GeV}}{\text{km eV}^2} \right), \tag{1}$$

where Δm^2 is $|m_1^2 - m_2^2|$, α is the mixing angle, E_ν is the neutrino energy, and L is the distance the neutrino travels between production and observation. Nonzero neutrino mass and mixing would have important implications for cosmology and particle physics. Neutrino oscillations may explain observed neutrino deficits from the sun and from cosmic ray sources. Accelerator experiments will continue the search for neutrino mixing with particular emphasis on the tau sector [1] [2].

To date the best limits for $\nu_\mu \rightarrow \nu_\tau$ oscillations are derived from searches for ν_τ appearance through exclusive processes. For example, the E531 limit [3] comes from searching for a detached vertex from a tau decay in emulsion. A fine grained detector (*i.e.* emulsion, or a low density fine grained calorimeter such as was used by CHARM II [4]) is necessary to be sensitive to low mixing angles through exclusive modes.

In this report, we obtain results with comparable sensitivity to E531 and CHARM II using the massive and relatively coarse grained CCFR detector. The main advantage of this type of detector is statistical power which will be particularly important in a low flux, long baseline neutrino beam [2]. Our result establishes the sensitivity of such detectors to small mixing angles.

The CCFR detector [5] consists of an 18 m long, 690 ton target calorimeter with a mean density of 4.2 g/cm^3, followed by an iron toroid spectrometer. The target calorimeter consists of 168 iron plates, 3m $\times$ 3m $\times$ 5.1cm each. The active elements are liquid scintillation counters spaced every two plates and drift chambers spaced every four plates. There are a total of 84 scintillation counters and 42 drift chambers in the target. The toroid spectrometer is not directly used in this analysis.

The Tevatron Quadrupole Triplet neutrino beam is created by decays of pions and kaons
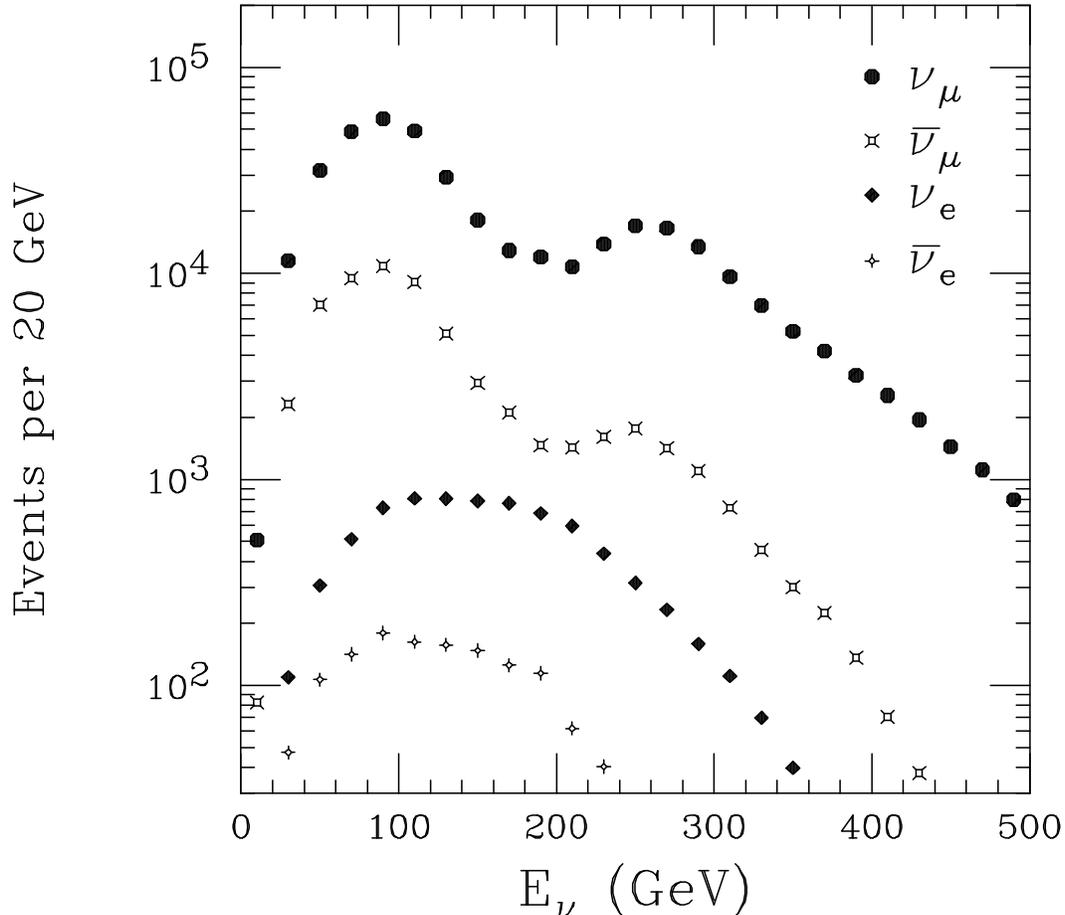
3

FIG. 1. Neutrino energy spectra for ν_μ, $\overline{\nu}_\mu$, ν_e, and $\overline{\nu}_e$ at the CCFR detector for the FNAL wideband neutrino beam. (Monte Carlo based on measured relative ν_μ and $\overline{\nu}_\mu$ fluxes).

produced when 800 GeV protons hit a production target. A wide band of secondary energies is accepted by focusing magnets. The production target is located about 1.4 km upstream of the neutrino detector. The production target and focusing train are followed by a 0.5 km decay region. The resulting neutrino energy spectra for ν_μ, $\overline{\nu}_\mu$, ν_e, and $\overline{\nu}_e$ at the detector are shown in Figure 1. The beam contains a 2.3% fraction of electron neutrinos and a negligible fraction of tau neutrinos (less than 10^{-5}) which result primarily from D_s decay.

Neutrinos are observed in the target calorimeter *via* their neutral current and charged current interactions. Charged current events are characterized by the presence of a muon in the final state which deposits energy in a large number of consecutive scintillation counters as it travels through the calorimeter. Neutral current events have no muon and deposit energy over a range of counters typical of a hadronic shower (5 to 20 counters). Accordingly,

we define "short" events as those which deposit energy over an interval of 30 or fewer scintillation counters. The ratio R_{30} is defined to be the number of short events divided by the number of long events [6]. This ratio is strongly dependent on the ratio of neutral to charged current events which is a function of the electroweak mixing angle, $\sin^2\theta_W$.

Assuming the validity of the Standard Model, $\sin^2\theta_W$ is accurately measured from other processes. We can use these measurements to predict the ratio of neutral to charged current events in the CCFR detector, and thus R_{30}. The presence of ν_τ in the neutrino beam would cause the measured R_{30} to be larger than its calculated value because most charged current tau neutrino interactions do not produce a muon in the final state and will thus appear "short".

In this result, we attribute any deviation in our measured R_{30} from the predicted value to $\nu_\mu \to \nu_\tau$ oscillations. As has been discussed in Ref. [7], this technique is also sensitive to $\nu_\mu \to \nu_e$. By assuming that only a single process ($\nu_\mu \to \nu_\tau$) contributes, the oscillation limit is conservative since any $\nu_\mu \to \nu_e$ oscillation would also increase the measured R_{30}.

We used a detailed Monte Carlo to relate a given $\nu_\mu \to \nu_\tau$ oscillation probability to the quantity R_{30}. The $\sin^2\theta_W$ value[1] in the on-shell renormalization scheme of 0.2232 ± 0.0018 is input to the Monte Carlo. The other inputs to the Monte Carlo are parameterizations of the measured CCFR detector responses [5], nucleon structure functions [12], and relative neutrino beam fluxes extracted from the charged current data sample [13]. The ν_e flux is modeled in a detailed beamline simulation, normalized by the observed ν_μ flux [6]. The same beamline simulation is used to tag the decay location for each pion and kaon and thus

---

[1]This value for $\sin^2\theta_W$ is obtained using the world average value M_W measurement [8], the prediction from the measured M_Z, and the average of all LEP and SLD Z-pole measurements from [9]. The M_Z extraction is corrected for the recent re-evaluation of $\alpha_{EM}(M_Z^2)$ by Swartz [10]. A top mass of 180 ± 12 GeV [11] and $60 < M_{\text{Higgs}} < 1000$ GeV are used to convert from the $\overline{\text{MS}}$ and M_Z schemes to the on-shell scheme used here.

the creation point of each ν_μ along the beamline. The measured flux gives the number of ν_μ's at the detector. $P(\nu_\mu \to \nu_\tau)$ is determined from Eq. 1 and the beamline simulation. We assume $P(\nu_\mu \to \nu_\tau) = P(\overline{\nu}_\mu \to \overline{\nu}_\tau)$ (a consequence of CP invariance). The number of ν_μ's produced in the beamline is then the number observed at the detector divided by $1 - P(\nu_\mu \to \nu_\tau)$. The electron neutrino flux is rescaled to the *produced* number of ν_μ's. The tau neutrino flux is calculated by multiplying the *produced* number of ν_μ's by $P(\nu_\mu \to \nu_\tau)$.

To simulate ν_τ interactions in our detector we assumed the ν_τ neutral current cross section is the same as for ν_μ interactions. The ν_τ charged current cross section was calculated including mass suppression terms. Following [14] we used the approximation that the structure functions $F_4 = 0$, and $xF_5 = 2xF_1$. The kinematic suppression for massive particle production was also taken into account. The Monte Carlo program TAUOLA [15] was used to simulate tau decays. We define E_{cal} as the energy deposited in the calorimeter in the first twenty counters following the event vertex. For ν_τ charged current events E_{cal} includes the visible energy from the tau decay. Events are required to deposit a minimum energy of 30 GeV in the target calorimeter. The contributions from quasi-elastic and resonance production are suppressed by this requirement.

Events were selected using a calorimeter trigger fully sensitive for E_{cal} above 20 GeV. To ensure event containment, the fiducial volume of the detector is limited to a central cylindrical region 30" in radius and excludes events which began in the first 6 counters or the last 34 counters of the detector. The resulting data sample consisted of about 450,000 events. The data and Monte Carlo are divided into 21 E_{cal} bins. For each Δm^2, the Monte Carlo prediction for $R_{30}(E_{cal}, \sin^2 2\alpha)$ is compared with $R_{30}(E_{cal})$ from the data. Figure 2 shows the R_{30} distribution as a function of E_{cal} for the data and for the Monte Carlo simulation. The detailed shape of $R_{30}(E_{cal})$ depends on many competing effects which are put into the Monte Carlo, but is dominated by the variation of short charged current events with E_{cal} and by the contribution from the ν_e flux.

There are four major uncertainties in the comparison of $R_{30}(E_{cal})$ from the Monte Carlo to the data: the statistical error in the data, the uncertainty in the effective charm quark
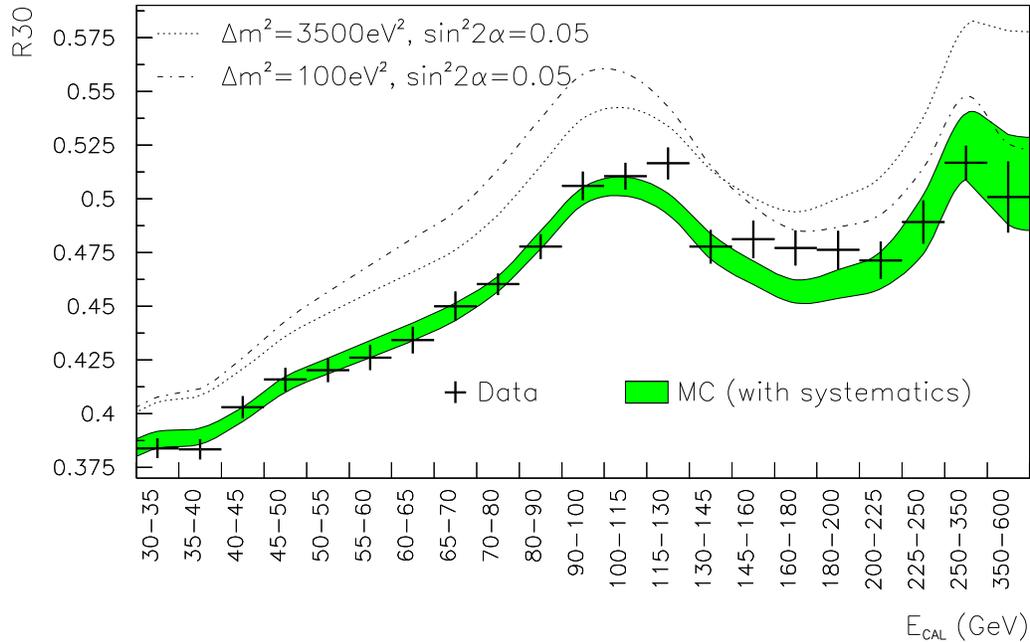
6

FIG. 2. R_{30} as a function of E_{cal} for the data (points). The filled band shows Monte Carlo assuming no oscillations with 1σ systematic errors added in quadrature. Data points show statistical errors only. The dotted curve corresponds to $\Delta m^2 = 3500$ eV^2 and $\sin^2 2\alpha = 0.05$ and the dashed curve to $\Delta m^2 = 100$ eV^2 and $\sin^2 2\alpha = 0.05$. The curve for $\Delta m^2 = 100$ eV^2 corresponds to lower energy neutrinos for which less energy is deposited in the calorimeter. At high Δm^2 the high E_{cal} events are most sensitive to ν_τ appearance.

Source of Error	$\Delta m^2 = 3500$ eV^2	310 eV^2	80 eV^2
statistical	2.4×10^{-3}	1.8×10^{-3}	2.1×10^{-3}
ν_e beam content	2.5×10^{-3}	2.0×10^{-3}	1.4×10^{-3}
detector systematics	2.2×10^{-3}	2.0×10^{-3}	2.0×10^{-3}
charm mass	2.4×10^{-3}	1.6×10^{-3}	2.4×10^{-3}
charm sea	1.2×10^{-3}	0.8×10^{-3}	1.0×10^{-3}
$\sin^2 \theta_W$	1.7×10^{-3}	1.2×10^{-3}	1.5×10^{-3}
other model	0.6×10^{-3}	0.6×10^{-3}	0.7×10^{-3}
Total	5.2×10^{-3}	4.1×10^{-3}	4.4×10^{-3}

TABLE I. The change in $\sin^2 2\alpha$ from a one sigma shift in the dominant errors. The row labeled "total" includes these and many smaller uncertainties added in quadrature.

mass for charged current charm production, the uncertainty in the incident flux of ν_e's on the detector, and the uncertainty in the on-shell weak mixing angle from outside measurements. Other sources of systematic uncertainty were also investigated [6]. Table I shows the effect of the uncertainties for three choices of Δm^2.

The charm mass error comes from the uncertainty in modeling the turn-on of the charm quark production cross section. The Monte Carlo uses a slow-rescaling model with the parameters extracted using events with two oppositely charged muons in this experiment [16]. This error dominates the calculation of R_{30} at low E_ν (and low E_{cal}) where the threshold suppression is greatest. The ν_e flux uncertainty has a large effect on R_{30} because almost all charged current ν_e events are short events. Therefore, the relatively small (4.2%) fractional uncertainty in the ν_e flux is a large effect, particularly at high E_{cal} since most ν_e charged current interactions deposit the full incident neutrino energy into the calorimeter.

The data are fit by forming a χ^2 function given by:

$$\chi^2 = \sum_{\text{systematics}} C_i^2$$

$$+ \sum_{\mathrm{E_{cal}}} \left(\frac{\mathrm{Data}(E_{\mathrm{cal}}) - \mathrm{MC}(E_{\mathrm{cal}}; \Delta m^2, \sin^2 2\alpha; C_i)}{\sigma_{\mathrm{stat}}} \right)^2 .$$

This incorporates the Monte Carlo generated effect of the oscillations as well the effect of the systematic errors. The systematic coefficients, C_i, represent deviations of systematic effects from their nominal value in units of systematic sigmas. A best fit $\sin^2 2\alpha$ is determined for each Δm^2 by minimizing the χ^2 as a function of $\sin^2 2\alpha$ and the 33 systematic coefficients, C_i. Best fit values of $\sin^2 2\alpha$ with one sigma errors from the fit are shown in Table II. At all Δm^2, the data are consistent with no observed $\nu_\mu \rightarrow \nu_\tau$ oscillation. The statistical significance of the best-fit oscillation at any Δm^2 is at most 1.2 sigma.

The frequentist approach [17] is used to set a 90% confidence upper limit for each Δm^2. The limit in $\sin^2 2\alpha$ at each Δm^2 corresponds to a shift of 1.64 units of $\chi^2(\sin^2 2\alpha)$ from the minimum χ^2 (at the best fit value in Table II). The χ^2 value for the no-oscillations case is 15.7/21 dof. The 90% confidence upper limit is plotted in Figure 3. The best limit of $\sin^2 2\alpha < 2.7 \times 10^{-3}$ is at $\Delta m^2 = 50$ eV^2. For $\sin^2 2\alpha = 1$, $\Delta m^2 > 1.4$ eV^2 is excluded, and for $\Delta m^2 \gg 1000$ eV^2, $\sin^2 2\alpha > 8.1 \times 10^{-3}$ is excluded at 90% confidence.

This result demonstrates sensitivity to low mixing angles in a high mass, coarse grained sampling calorimeter and has implications for proposed long-baseline experiments [2]. However, a detailed Monte Carlo study of the sensitivity of those experiments must be performed to correctly apply this result. The lower energy and the lower level of statistics in the long baseline experiments will result in less statistical sensitivity, while having both a near and far detector would reduce many of the other sources of uncertainty [18] listed in Table I.

In conclusion, we have used a new analysis method to search for $\nu_\mu \rightarrow \nu_\tau$ oscillations. We see a result consistent with no neutrino oscillation and find a 90% confidence level excluded region in $\sin^2 2\alpha$-Δm^2 space. This result is the most stringent limit to date for $25 < \Delta m^2 < 90$ eV^2, and is comparable to those from E531 [3], and from CHARM II [4], which were obtained using fine grained detectors.

Δm^2 (eV^2)	Best Fit	Sigma	Δm^2 (eV^2)	Best Fit	Sigma
2.0	-2.1114	2.0192	185.0	0.0050	0.0042
3.5	-0.6982	0.6676	200.0	0.0047	0.0042
5.0	-0.3419	0.3268	220.0	0.0040	0.0041
6.0	-0.2373	0.2267	240.0	0.0033	0.0041
8.0	-0.1351	0.1296	275.0	0.0022	0.0040
10.0	-0.0872	0.0838	295.0	0.0018	0.0040
15.0	-0.0397	0.0385	310.0	0.0016	0.0040
20.0	-0.0229	0.0224	350.0	0.0010	0.0041
35.0	-0.0084	0.0090	400.0	0.0002	0.0043
42.0	-0.0061	0.0069	430.0	-0.0002	0.0044
50.0	-0.0045	0.0056	500.0	-0.0002	0.0047
60.0	-0.0031	0.0047	550.0	0.0004	0.0048
70.0	-0.0021	0.0041	600.0	0.0013	0.0050
80.0	-0.0013	0.0038	650.0	0.0020	0.0051
90.0	-0.0006	0.0036	700.0	0.0026	0.0051
100.0	0.0001	0.0035	750.0	0.0028	0.0050
110.0	0.0008	0.0035	800.0	0.0027	0.0049
120.0	0.0015	0.0036	1000.0	0.0017	0.0049
135.0	0.0027	0.0037	2000.0	0.0018	0.0050
150.0	0.0038	0.0039	3500.0	0.0018	0.0049
175.0	0.0049	0.0041	10000.0	0.0018	0.0049

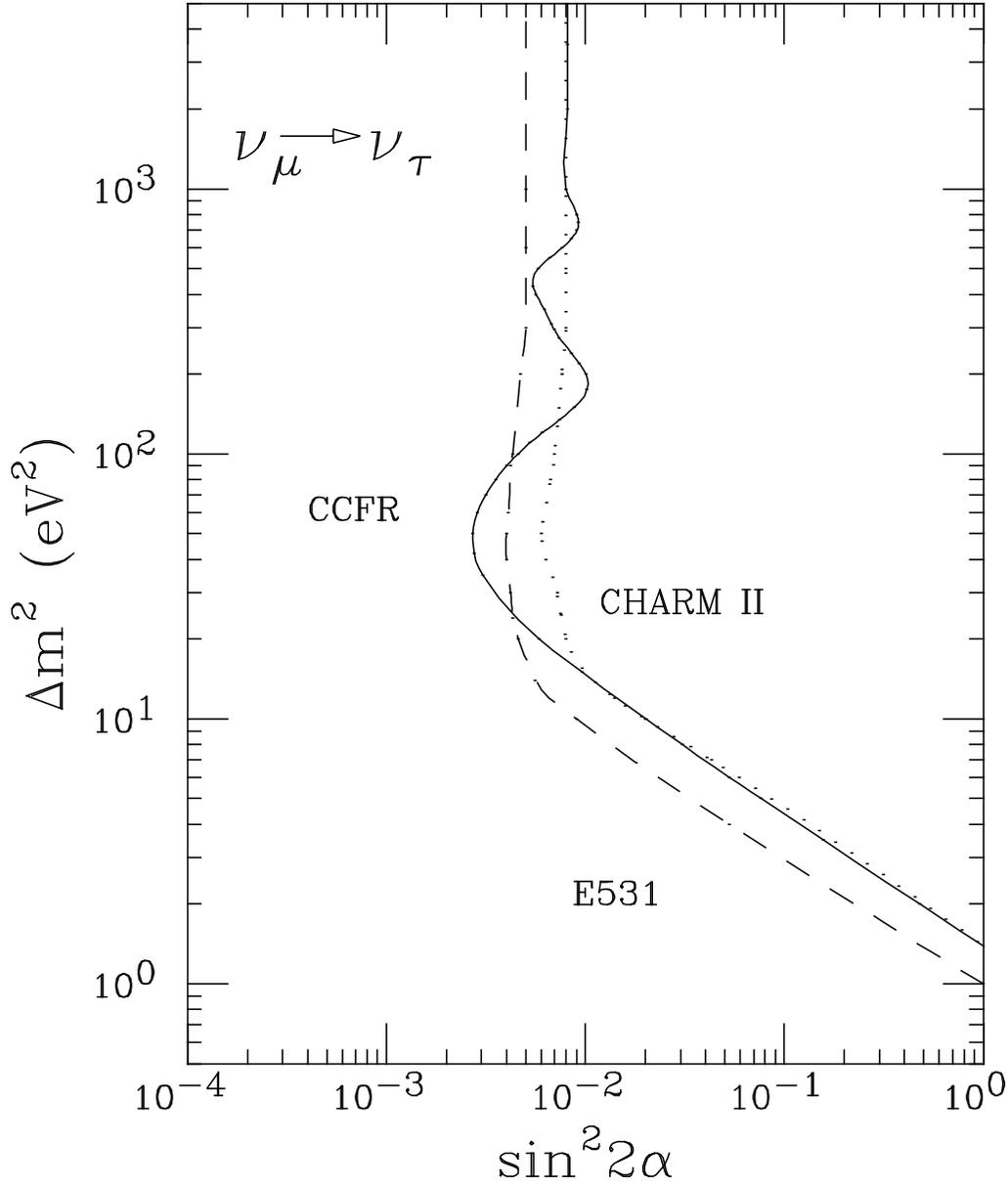TABLE II. The result for $\sin^2 2\alpha$ from the fit at each Δm^2

FIG. 3. Excluded region of $\sin^2 2\alpha$ and Δm^2 from this analysis at 90% confidence is shown as a solid curve. Also shown are the same results from E531 (dashed curve), and CHARM II (dotted).

REFERENCES

[1] K. Kodama *et al* , Fermilab proposal P-803 October (1994); A. K. Mann *et al* , Brookhaven AGS Proposal P-889, August 1992; CHORUS collaboration, CERN-SPSC/90-42(1990); NOMAD collaboration, CERN-SPSLC/92-51(1992).

[2] E. Ables *et al* , Fermilab proposal P-875 (MINOS), February (1995).

[3] N. Ushida *et al* , Phys. Rev. Lett. **57**, 2897 (1986).

[4] M. Gruwe *et al* , Phys. Lett. **B309**, 463 (1993).

[5] W. K. Sakumoto *et al* , Nucl. Instrum. Methods **A294**,179 (1990); B. J. King *et al* , Nucl. Instrum. Methods **A302**,254 (1991).

[6] C. Arroyo *et al* , Phys. Rev. Lett. **72**, 3452, (1994); Bruce J. King, PhD Thesis, Columbia University (1994), Nevis preprint 284, unpublished.

[7] P.F. Loverre, Phys. Lett. **B206**, 711 (1988).

[8] F. Abe *et al* FERMILAB-PUB-95/033-E (1995).

[9] P. Langacker, Particle Data Group, Phys. Rev. **D50**,1309 (1994).

[10] M. L. Swartz, SLAC-PUB-6711 (1994).

[11] F. Abe *et al* FERMILAB-PUB-95/022-E (1995); S. Abachi *et al* FERMILAB-PUB-95/028-E (1995).

[12] P.Z. Quintas *et al* , Phys. Rev. Lett. **71**, 1307 (1993), W.C. Leung *et al* , Phys Lett. **B317**, p.655 (1993).

[13] P.Z. Quintas, PhD Thesis, Columbia University (1992), Nevis Preprint 277, unpublished, W.C. Leung, PhD Thesis, Columbia University (1991), Nevis Preprint 276, unpublished.

[14] C.H. Albright and C. Jarlskog, Nuc. Phys. **B84**, 467 (1975).

[15] S. Jadach *et al* , Comput. Phys. Comm. **64**, 275 (1991).

[16] A. O. Bazarko *et al* , Z. Phys. C., **65** 189 (1995).

[17] Particle Data Group, Phys. Rev. **D50**,1280 (1994).

[18] R. H. Bernstein and S. J. Parke, Phys. Rev. **44** 2069 (1991).